

RESEARCH ARTICLE

MiR-221-3p and miR-92a-3p enhances smoking-induced inflammation in COPD

Yahui Shen¹ | Huiyu Lu¹ | Guixian Song² 

¹Department of Respiratory and Critical Care Medicine, Taizhou Clinical Medical School of Nanjing Medical University (Taizhou People's Hospital), Taizhou, China

²Department of Cardiology, Taizhou Clinical Medical School of Nanjing Medical University (Taizhou People's Hospital), Taizhou, China

Correspondence

Guixian Song, Department of Cardiology, Taizhou Clinical Medical School of Nanjing Medical University (Taizhou People's Hospital), No. 366 Taihu Road, 225300 Taizhou City, Jiangsu Province, China. Email: songguixianey@yeah.net

Funding information

This study was supported by Jiangsu Provincial Medical Youth Talent (QNRC2016511, QNRC2016512) and Taizhou Municipal Science and Technology Bureau (TS201729)

Abstract

Background: Smoking is likely to facilitate airway inflammation and finally contributes to chronic obstructive pulmonary disease (COPD). This investigation was intended to elucidate miRNAs that were involved in smoking-induced COPD.

Methods: Altogether 155 COPD patients and 77 healthy volunteers were recruited, and their serum levels of miR-221-3p and miR-92a-3p were determined. Besides, human bronchial epithelial cells (16HBECs) were purchased, and they were treated by varying concentrations of cigarette smoke extract (CSE). The 16HBECs were, additionally, transfected by miR-221-3p mimic, miR-92a-3p mimic, miR-221-3p inhibitor or miR-92a-3p inhibitor, and cytokines released by them, including TNF- α , IL-8, IL-1 β , and TGF- β 1, were monitored using enzyme linked immunosorbent assay (ELISA) kits.

Results: Chronic obstructive pulmonary disease patients possessed higher serum levels of miR-221-3p and miR-92a-3p than healthy volunteers ($p < 0.05$), and both miR-221-3p and miR-92a-3p were effective biomarkers in diagnosing stable COPD from acute exacerbation COPD. Moreover, viability of 16HBECs was undermined by CSE treatment ($p < 0.05$), and exposure to CSE facilitated 16HBECs' release of TNF- α , IL-8, IL-1 β , and TGF- β 1 ($p < 0.05$). Furthermore, miR-221-3p/miR-92a-3p expression in 16HBECs was significantly suppressed after transfection of miR-221-3p/miR-92a-3p inhibitor ($p < 0.05$), which abated CSE-triggered increase in cytokine production and decline in viability of 16HBECs ($p < 0.05$).

Conclusion: MiR-221-3p and miR-92a-3p were involved in CSE-induced hyperinflammation of COPD, suggesting that they were favorable alternatives in diagnosing COPD patients with smoking history.

KEYWORDS

chronic obstructive pulmonary disease, cigarette smoke extract, diagnosis, inflammation, miR-221-3p, miR-92a-3p

1 | INTRODUCTION

Smoking, widely acknowledged as an essential trigger of chronic obstructive pulmonary disease (COPD), is likely to seriously injure

mucous membrane of respiratory tract and finally give rise to lung malfunction.¹ It has been confirmed that smoking-induced COPD is tightly linked with inflammatory dysregulation, immunity imbalance, and oxidative stress,² for instance, inflammation biomarkers,

This is an open access article under the terms of the Creative Commons Attribution-NonCommercial-NoDerivs License, which permits use and distribution in any medium, provided the original work is properly cited, the use is non-commercial and no modifications or adaptations are made.

© 2021 The Authors. *Journal of Clinical Laboratory Analysis* published by Wiley Periodicals LLC

including nuclear factor κ B (NF- κ B), tumor necrosis factor alpha (TNF- α), matrix metalloproteinases (MMPs), C-reactive protein (CRP), and interleukins (ILs), are usually up-regulated in the serum of COPD patients.³⁻⁵ It is, however, insufficient to diagnose COPD merely through tracking level changes of the biomarkers, which might engender delays in COPD treatment. To avoid over/under diagnosis/treatment of COPD, it is paramount to clarify mechanisms of smoking-induced COPD at the genetic level, which might precede histopathological damages in the trachea of COPD patients.

MiRNAs, stably expressed in serum, are reported to signalize patho-physiological changes of inflammation diseases sensitively.⁶ For example, miR-221 was discovered to activate MAPK signaling and NF- κ B signaling, both of which are responsible for over-inflammation in COPD.⁷⁻¹⁰ More than that, miR-221 level was elevated in human umbilical vein endothelial cells (HUVECs) exposed to TNF- α ,¹¹ and its rise enhanced secretion of IL-6, TNF- α , and IL-1 β , whose levels were heightened as COPD severity escalated,^{12,13} by targeting SIRT1 in the context of diabetes mellitus.¹⁴ With respect to miR-92a, a member of miR-17-92 family, restraint of its level markedly diminished endothelial inflammation strengthened by oxidized low-density lipoprotein (oxLDL),¹⁵ besides involvements in coronary artery lesion, vascular endothelial injury and tumorigenesis.¹⁶⁻¹⁸ Similar to miR-221, miR-92a also participated in exacerbating inflammation via promoting NF- κ B signaling, albeit in diabetes mellitus-related cardiovascular disease.¹⁹ Despite pronounced roles in the inflammation disorders, the involvement of miR-221 and miR-92a in controlling inflammation of smoking-induced COPD remained vague.

Therefore, this investigation attempted to elucidate the performance of miR-221-3p and miR-92a-3p in diagnosing COPD of varying severities, and also to evaluate their associations with inflammation dysfunction underlying etiology of smoking-triggered COPD.

2 | MATERIALS AND METHODS

2.1 | Inclusion of COPD patients

One hundred and fifty-five COPD patients, grouped into patients with stable COPD ($n = 71$) and patients with acute exacerbation (ae)-COPD ($n = 84$), and 77 healthy people (control group) who conducted physical examination were recruited from Taizhou Clinical Medical School of Nanjing Medical University. Patients under following circumstances were incorporated into stable COPD group: 1) they hardly demonstrated any cough- or sputum-related syndromes for >1 month; 2) they received no other treatment except inhalation of bronchodilators/glucocorticoids for 1 month; and 3) they had a smoking history of >5 years. The participants were excluded from stable COPD group if they: 1) concurrently suffered from severe disorders in heart, brain, liver, and kidney; 2) they were accompanied by other systemic chronic diseases; 3) were

tumor patients; 4) inhaled glucocorticoid for a long term; and 5) performed mechanical ventilation. Moreover, ae-COPD patients were included if: 1) they were newly admitted, and their cough/sputum deteriorated within 1 week; 2) they inhaled bronchodilators/glucocorticoids for >1 month; and 3) they had smoked for >5 years. Correspondingly, the ae-COPD patients were excluded in case that: (1) they were accompanied by pneumothorax, rib fracture, cardiovascular/cerebrovascular diseases, infection, severe dysfunctions in liver and kidney, or other respiratory diseases; and (2) they were plagued by respiratory infection for >1 month. Furthermore, the COPD patients were grouped in accordance with their severity, by consulting standards set by Global Initiative for Chronic Obstructive Lung Disease (GOLD).²⁰ All participants have signed informed consents, and this program was approved by Taizhou Clinical Medical School of Nanjing Medical University and the ethics committee of Taizhou Clinical Medical School of Nanjing Medical University (KY201904701). What's more, 3 ml cubital venous blood was collected from each COPD patient and healthy participant, and the blood samples were stored at -80°C after being centrifuged at the speed of 3,000 r/min.

2.2 | Acquisition of cigarette smoke extracts (CSE)

Following procedures stated by Krimmer et al.,²¹ two filter-tipped cigarettes (brand: Daqianmen, Shanxi Taiyuan Tobacco company, China), including 0.013G tar, 0.001g nicotine, and 0.014g carbon monoxide per cigarette, were ignited, and the gas collected by negative pressure suction was injected through 100 ml RPMI-1640 serum-free medium (Gibco, USA). The products were stored at 4°C in a sealed bottle.

2.3 | Cell culture

Human bronchial epithelial cells (16HBECs), purchased from American Type Culture Collection (ATCC) (USA), were inoculated into 10% fetal bovine serum (FBS) (Gibco, USA)-containing RPMI-1640 complete medium (Gibco, USA). They were cultured in an incubator of 5% CO_2 and saturated humidity at the constant temperature of 37°C .

2.4 | Cell transfection

Precisely 1×10^6 16HBECs were inoculated into each well of 6-well plates, and they were grown to 50-70% confluency. Then miR-221-3p mimic (4 μg , 5'-AGCUACAUUGUCUGCUGGGUUUC-3'), miR-221-3p inhibitor (4 μg , 5'-GAAACCCAGCAGACAAUGUAGCU-3'), miR-92a-3p mimic (4 μg , 5'-UAUUGCACUUGUCCGGCCUGU-3'), miR-92a-3p inhibitor (4 μg , 5'-AUAACGUGAACAGGGCCGGACA-3') and miR-NC (4 μg , 5'-UUGUACUACACAAAAGUACUG-3') (Ribobio, China) were transfected into 16HBECs for 48 h, following the specification of Lipofectamine 2000 reagent kit (Invitrogen, USA).

TABLE 1 Comparison of baseline clinical characteristics between COPD patients and healthy people

Clinic characteristics	Acute exacerbation COPD	Stable COPD	Healthy control	F/ χ^2 /t test	p value
Number	84	71	77		
Age (year)	64.82 ± 6.18	63.54 ± 6.73	65.29 ± 7.31	1.33	0.268
Gender					
Male	55	40	37		
Female	29	31	40	4.99	0.083
Course	12.41 ± 3.06	11.73 ± 3.54		1.28	0.202
BMI (Kg/m ²)	23.58 ± 2.39	23.16 ± 3.55	22.89 ± 2.27	1.28	0.280
Smoking history					
With	84	71	35		
Without	-	-	42		
GOLD classification					
Stage I	8	12			
Stage II	23	25			
Stage III	29	20			
Stage IV	24	14		4.11	0.250
FVC (L)	1.61 ± 0.31	2.03 ± 0.61	2.81 ± 0.59	111.70	<0.001
FEV1 (L)	1.13 ± 0.18	1.73 ± 0.21	2.66 ± 0.18	1,319.00	<0.001
FEV1/FVC (%)	39.06 ± 4.82	61.73 ± 6.12	86.26 ± 7.55	1,154.00	<0.010

Abbreviations: BMI, body mass index; COPD, chronic obstructive pulmonary disease; FEV1, forced expiratory volume in 1 s; FVC, forced vital capacity.

2.5 | Real-time fluorescence quantitative polymerase chain reaction (qPCR)

Total RNAs were extracted from serum samples of subjects and 16HBECs by addition of Trizol reagent (Invitrogen, USA). Subsequently, miRNAs were isolated from total RNAs according to requirements of mirPremier[®] microRNA Isolation Kit (Bio-Rad, USA), and they were reversely transcribed into cDNAs utilizing SuperScript RT Kit (Dalian Baosheng, China). Real-time PCR of the cDNAs was accomplished with the aid of SYBR Green PCR master Mix kit (Dalian Baosheng, China), abiding by steps as below: 1) pre-denaturation at 95°C for 30 s, and 2) 40 cycles of denaturation at 95°C for 5 s, annealing at 60°C for 30 s and extension at 70°C for 10 s. Finally, expressions of miR-221-3p and miR-92a-3p were quantified by means of 2^{-ΔΔCt} method, and they were normalized to expression of U6.

2.6 | Enzyme-linked immunosorbent assay (ELISA)

Tumor necrosis factor alpha, IL-6, IL-1β and TGF-β1 levels in the serum of participants and in the supernatant of 16HBECs were measured according to detailed guidance of separate ELISA kits (Shenzhen Jingmei Biotech, China).

2.7 | Western blotting

After supplementation of 1% phenylmethylsulfonyl fluoride (PMSF)-containing RIPA lysate (Sigma, USA), total proteins were dissociated from 16HBECs, and the amount of proteins was determined through BCA method (Beyotime, China). Every 50 μg protein in each treatment group

was collected to implement sodium dodecyl sulfate-polyacrylamide gel electrophoresis (SDS-PAGE) (Beyotime, China), products of which were transferred onto polyvinylidene fluoride (PVDF) membrane (Millipore, USA) by wet method. Then protein samples under each treatment were blocked by 5% skimmed milk for 1 h, after which they were incubated by primary antibodies (mouse anti-human, Abcam, USA) against Collagen IV (cat. no.: ab86042, 1:1000), Fibronectin (cat. no.: ab253288, 1:500), α-SMA (cat. no.: ab119952, 1:2000) and GAPDH (cat. no.: ab8245, 1:1000) at 4°C for overnight. After rinsing the PVDF membrane with Phosphate Buffered Saline with Tween (PBST), the samples were incubated with Goat Anti-Mouse IgG H&L (cat. no.: ab47827, 1:5000, Abcam) for 2 h. Following 10-min development using electrochemiluminescence (ECL) reagent (Beyotime, China), photographs were taken through infrared laser imaging system (Odyssey, LI-COR Biosciences, USA). Relative expressions of Collagen IV, Fibronectin or α-SMA were assessed using Image-Pro Plus software (Media Cybernetics, USA), and GAPDH was designated as their internal reference.

2.8 | 3-(4,5-Dimethylthiazol-2-yl)-2,5-diphenyltetrazolium bromide (MTT) assay

After digestion by 0.25% pancreatin (Gibco, USA), 16HBECs of exponential growth phase were adjusted to the concentration of 5 × 10⁴ per ml. Until 16HBECs grew to 70%-80% confluence, 16HBECs in each well were blended by 200 μl CSE, which were diluted to ratios of 0%, 2.5%, 5.0%, 7.5% or 10.0% by supplementing serum-free minimum essential medium (MEM) culture medium (Gibco, USA). After 24 h of culture, 16HBECs in each well were treated by 20 μl MTT solution (Promega, USA) for 4 h, following which they were blended by 150 μl dimethylsulfoxide (DMSO) (Sino-American

Biotechnology, China). Absorbance (A) values of each well were detected at the wavelength of 490 nm, with the assistance of an automatic microplate reader (BioTek, USA).

2.9 | Cell apoptosis assay

After addition of 200 μ l Annexin V/Propidium Iodide (PI) staining solution (BD Bioscience, USA), the 16HBECs were incubated in the darkness for 15 min. Apoptotic rates of 16HBECs under each treatment were tested on the flow cytometer (BD Bioscience, USA), and excitation light wavelength of the instrument was fixed at 488 nm, with channel filters at 515 nm to detect Fluorescein isothiocyanate (FITC) fluorescence and channel filters at >560 nm to determine PI fluorescence.

2.10 | Colony formation assay

The 16HBECs at the logarithmic growth phase were inoculated into 24-well plates at the density of 500 per well after being digested by pancreatin. Ten days later, 16HBECs were fixed by methanol for 15 min and were stained by Giemsa for 20 min (Sigma-Aldrich, USA). Colonies that were made up of >50 16HBECs were counted under the microscope (Olympus, Japan).

2.11 | Statistical analyses

SPSS 13.0 statistical software (SPSS, USA) was adopted to conduct data analyses in this investigation. Measurement data (mean \pm standard deviation [SD]) were compared through student's

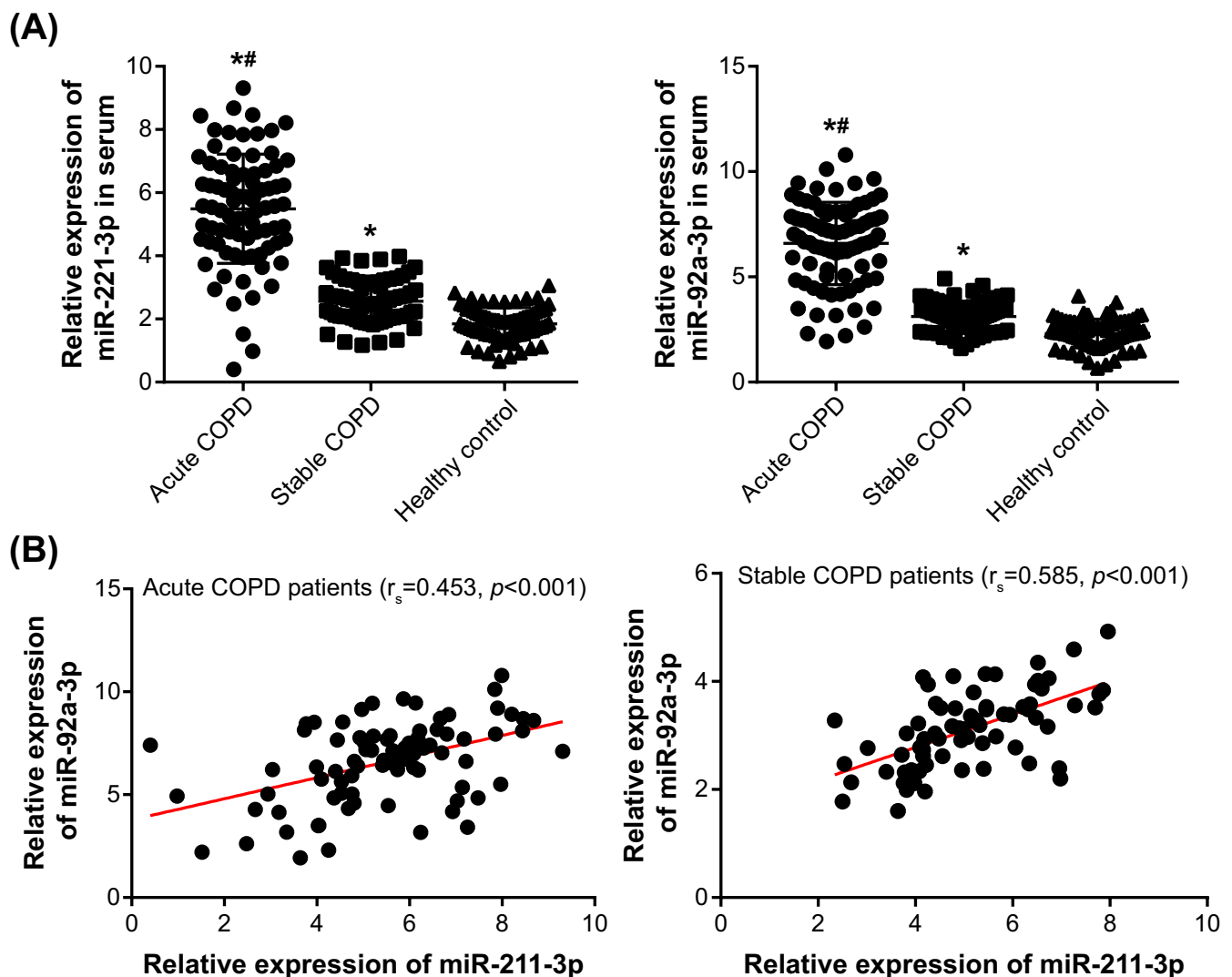


FIGURE 1 Association of miR-221-3p and miR-92a-3p with chronic obstructive pulmonary disease (COPD) onset. (A) Expressions of miR-221-3p and miR-92a-3p were determined in serum of patients with acute exacerbation COPD, patients with stable COPD and healthy volunteers. * $p < 0.05$ when compared with healthy volunteers; # $p < 0.05$ when compared with stable COPD. (B) Serum level of miR-221-3p was correlated with miR-92a-3p of patients with acute exacerbation COPD or with stable COPD

t test or one-way analysis of variance (ANOVA), while enumeration data (n) between groups were contrasted via chi-square test. Correlations between miR-221-3p/miR-92a-3p level and levels of biomarkers, which were indicative of pulmonary function, were carried out based on Pearson's correlation analysis. And two-sided P values less than 0.05 symbolized statistical significance in the differences.

3 | RESULTS

3.1 | Comparison of baseline features between COPD patients and healthy volunteers

Hardly any significant difference was found among patients of acute COPD group, patients of stable COPD group and healthy controls with smoking history, with respect to age, gender distribution, and body

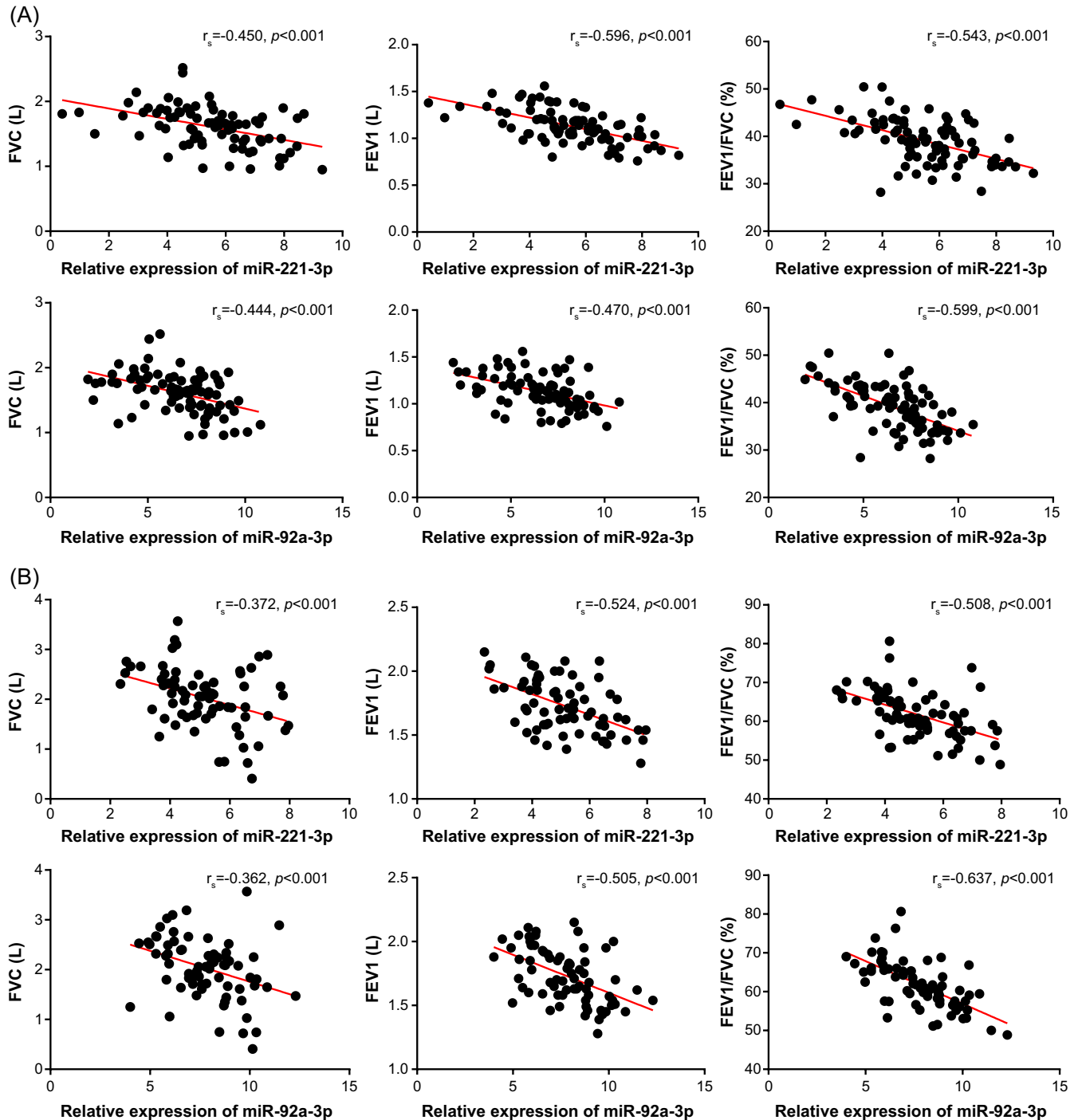


FIGURE 2 Correlation between serum level of miR-221-3p/miR-92a-3p and indicators of pulmonary function among patients with acute exacerbation COPD (A) and with stable COPD (B)

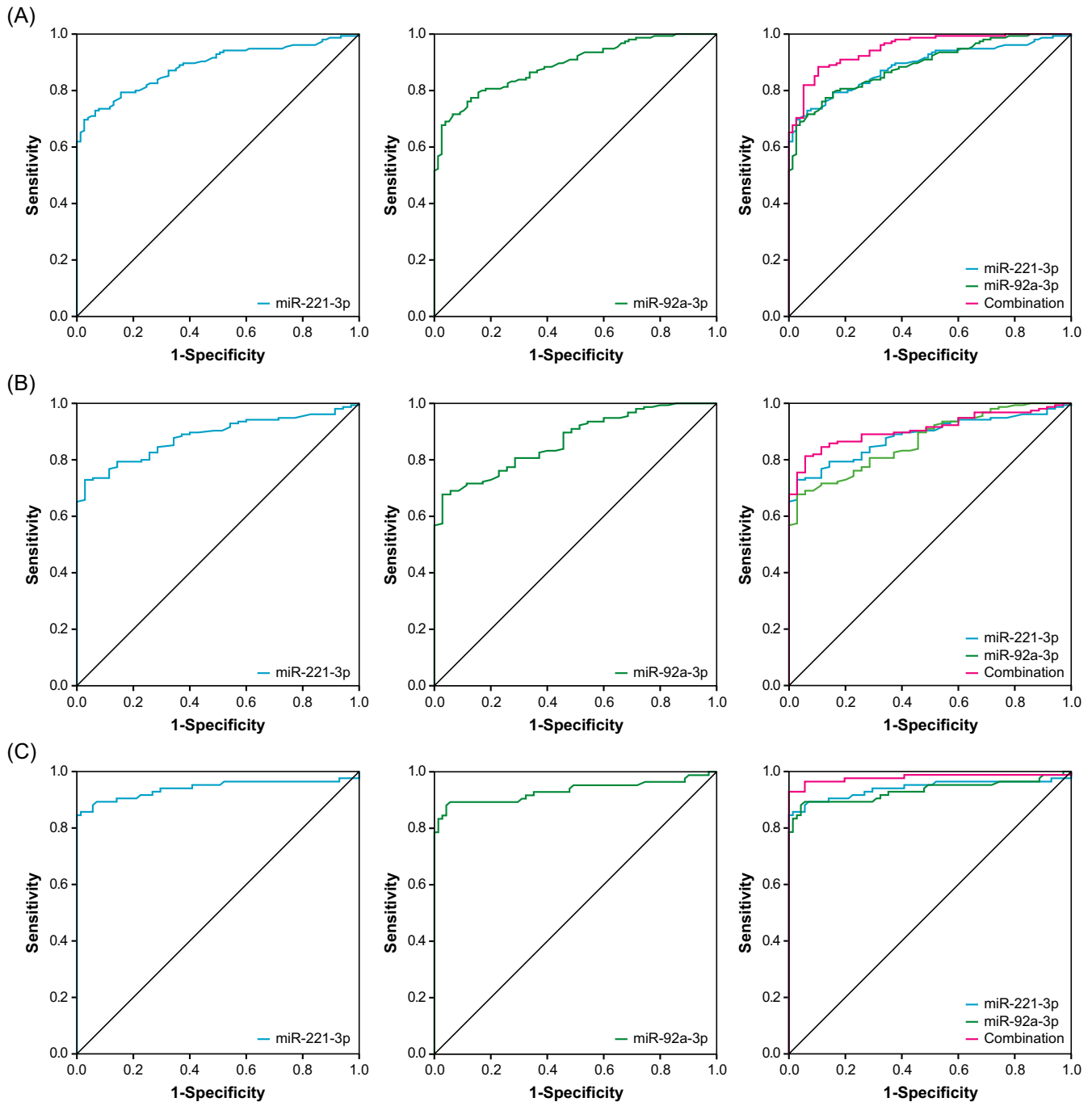


FIGURE 3 Diagnostic performances of miR-221-3p, miR-92a-3p and miR-221-3p&miR-92a-3p in diagnosing COPD patients from all healthy volunteers (A), in diagnosing COPD patients from healthy smokers (B), and in differentiating patients with acute exacerbation COPD from those with stable COPD (C)

mass index (BMI) ($p > 0.05$) (Table 1). Nevertheless, forced vital capacity (FVC), forced expiratory volume in 1 s (FEV1) and FEV1/FVC ratio were notably reduced in ae-COPD patients as relative to stable COPD patients ($p < 0.05$), and both of the COPD populations were associated with lower FVC, FEV1, and FEV1/FVC ratio than healthy volunteers with and without smoking history ($p < 0.05$) (Table 1). Moreover, serum levels of TNF- α , IL-6, IL-1 β , and TGF- β 1 were up-regulated in smokers with COPD, when compared with smokers without COPD (Figure S1A).

3.2 | Association of miR-221-3p/miR-92a-3p level with clinical features of COPD patients

Serum levels of miR-221-3p and miR-92a-3p went higher in ae-COPD patients than in stable COPD patients ($p < 0.05$), and COPD patients as a whole revealed higher serum levels of miR-221-3p and miR-92a-3p than healthy volunteers ($p < 0.05$) (Figure 1A). Furthermore, serum levels of miR-221-3p and miR-92a-3p tended to escalate in COPD patients at the advanced GOLD stage in comparison to

TABLE 2 Diagnostic performances of miR-221-3p, miR-91a-3p and its combination in differentiating COPD patients from healthy controls and Acute COPD patients from stable COPD patients

Groups	Biomarkers	Value	Sensitivity	Specificity	AUC	95% CI
COPD patients vs. healthy control	miR-221-3p	2.69	0.697	0.974	0.887	0.846–0.928
	miR-92a-3p	3.38	0.677	0.974	0.889	0.849–0.929
	miR-221-3p&miR-92a-3p	-	0.884	0.896	0.949	0.924–0.974
COPD patients vs. smokers in healthy control	miR-221-3p	2.59	0.729	0.971	0.883	0.835–0.930
	miR-92a-3p	3.38	0.677	0.971	0.867	0.814–0.920
	miR-221-3p&miR-92a-3p	-	0.813	0.943	0.909	0.868–0.950
Acute COPD patients vs. stable COPD patients	miR-221-3p	3.99	0.845	1.000	0.941	0.898–0.984
	miR-92a-3p	4.16	0.881	0.958	0.932	0.888–0.977
	miR-221-3p&miR-92a-3p	-	0.929	1.000	0.979	0.953–1.000

Abbreviations: AUC, area under the curve; CI, confidence interval; COPD, chronic obstructive pulmonary disease.

COPD patients at mild stages ($p < 0.05$) (Figure S1B). And smokers with COPD possessed higher serum levels of miR-221-3p and miR-92a-3p than smokers without COPD ($p < 0.05$) (Figure S1C). In addition, serum level of miR-221-3p was positively correlated with that of miR-92a-3p among patients with ae-COPD ($r_s = 0.453$) and stable COPD ($r_s = 0.585$) (Figure 1B), while serum levels of miR-221-3p and miR-92a-3p displayed negative correlations with FVC (ae-COPD: miR-221-3p $r_s = -0.450$, miR-92a-3p $r_s = -0.444$; stable COPD: miR-221-3p $r_s = -0.372$, miR-92a-3p $r_s = -0.362$), FEV1 (ae-COPD: miR-221-3p, $r_s = -0.596$, miR-92a-3p $r_s = -0.470$; stable COPD: miR-221-3p $r_s = -0.524$, miR-92a-3p $r_s = -0.505$) and FEV1/FVC ratio (ae-COPD: miR-221-3p $r_s = -0.543$, miR-92a-3p $r_s = -0.599$; stable COPD: miR-221-3p $r_s = -0.508$, miR-92a-3p $r_s = -0.637$) among ae-COPD patients and stable COPD patients (Figure 2).

3.3 | Diagnostic performance of miR-221-3p and miR-92a-3p for COPD

MiR-221-3p in combination with miR-92a-3p (AUC = 0.949) yielded superior performance in sorting out COPD patients from healthy volunteers as compared with when they were separately applied (miR-221-3p: AUC = 0.887; miR-92a-3p; AUC = 0.889) (Figure 3A, Table 2). MiR-221-3p (AUC = 0.941) and miR-92a-3p (AUC = 0.932) also seemed productive in diagnosing stable COPD patients from ae-COPD patients, and their combination resulted in an optimum AUC value of 0.979 (Figure 3C, Table 2). Furthermore, either miR-221-3p (AUC = 0.883) or miR-92a-3p (AUC = 0.867) was able to distinguish COPD patients, all of whom have smoking history, from smokers in the healthy control group, and their synergy showed more outstanding efficacy in this respect (AUC = 0.909) (Figure 3B, Table 2).

3.4 | Impact of CSE on miR-221-3p/miR-92a-3p expression, inflammation response and viability of 16HBECS

Viability of 16HBECS was depressed by increasing concentrations of CSE ($p < 0.05$), and this suppressive effect became prominent with

the prolongation of reaction time ($p < 0.05$) (Figure 4A). From the results, we intended to evaluate the impact of 2% CSE on 16HBECS, and the acting time was set as 48 h. It was indicated that miR-221-3p and miR-92a-3p were highly expressed in 2% CSE-treated 16HBECS in comparison to 16HBECS treated by none ($p < 0.05$) (Figure 4B), and apoptotic rate of 16HBECS in the CSE treatment group was around 2 folds of that in the NC group ($p < 0.05$) (Figure 4C). Expressions of TNF- α , IL-6, IL-1 β , TGF- β 1, Collagen IV, Fibronectin, and α -SMA were also significantly increased in 16HBECS of CSE treatment group, when compared with NC group ($p < 0.05$) (Figure 4D–E).

3.5 | Contribution of miR-221-3p/miR-92a-3p to viability, proliferation, apoptosis and inflammation response of 16HBECS

Viability and proliferation of 16HBECS were observably diminished in the CSE+miR-221-3p/miR-92a-3p mimic group as compared with CSE group, miR-221-3p mimic group and miR-92a-3p mimic group ($p < 0.05$), and 16HBECS of the latter 3 groups exhibited weaker viability and multiplicative potential than 16HBECS of NC group ($p < 0.05$) (Figure 5A–D). MiR-221-3p/miR-92a-3p inhibitor (ie, CSE+miR-221-3p/miR-92a-3p inhibitor group), to some degree, restored viability and proliferative ability of CSE-treated 16HBECS ($p < 0.05$) (Figure 5A–D). Moreover, apoptosis of 16HBECS in miR-221-3p mimic group, miR-92a-3p mimic group and CSE group was facilitated markedly as compared with NC group ($p < 0.05$), and miR-221-3p/miR-92a-3p mimic transfection cooperating with CSE treatment promoted 16HBECS apoptosis more significantly than CSE treatment alone ($p < 0.05$) (Figure 5E–F). However, miR-221-3p/miR-92a-3p inhibitor (ie, CSE+miR-221-3p/miR-92a-3p inhibitor group) partly reversed influence of CSE on apoptosis of 16HBECS ($p < 0.05$) (Figure 5E–F).

Furthermore, 16HBECS in miR-221-3p mimic group and miR-92a-3p mimic group expressed larger amounts of TNF- α , IL-6, IL-1 β , TGF- β 1, Collagen IV, Fibronectin, and α -SMA than NC group ($p < 0.05$), and dual treatments of CSE and miR-221-3p/miR-92a-3p mimic facilitated production of TNF- α , IL-6, IL-1 β , TGF- β 1, Collagen IV, Fibronectin, and α -SMA more dramatically than CSE treatment

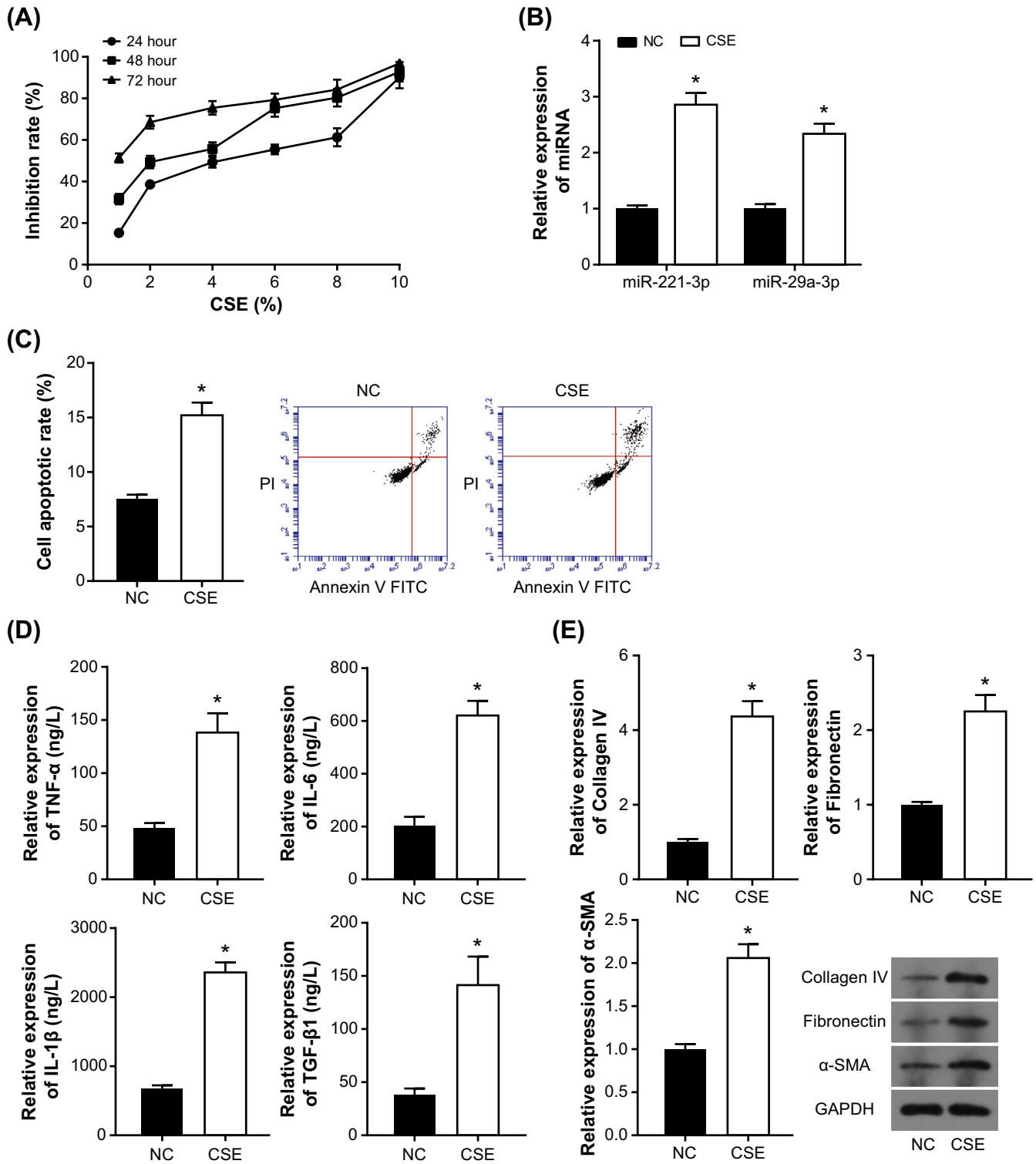


FIGURE 4 Impact of CSE on 16HBEc activity. (A) Inhibition of CSE on 16HBEc viability was determined under different concentrations. (B) Expressions of miR-221-3p and miR-92a-3p in 16HBEcs were detected after CSE treatment. * $p < 0.05$ when compared with NC group. (C) Apoptotic rate of 16HBEcs was evaluated after CSE treatment. * $p < 0.05$ when compared with NC group. (D) Expressions of TNF- α , IL-6, IL-1 β and TGF- β 1 were assessed after CSE treatment. * $p < 0.05$ when compared with NC group. (E) Expressions of Collagen IV, Fibronectin and α -SMA were measured after CSE treatment. * $p < 0.05$ when compared with NC group

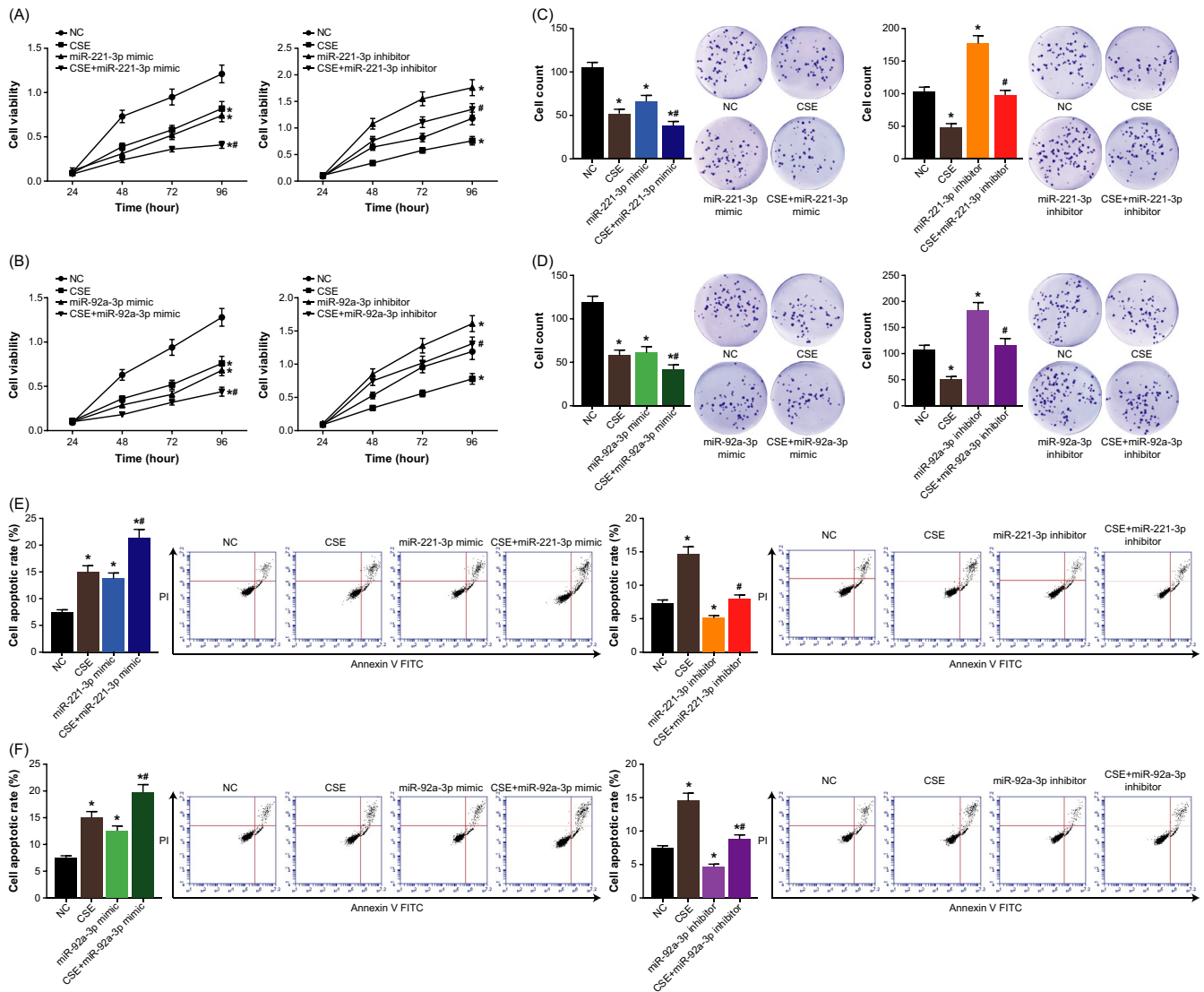


FIGURE 5 Viability (A–B), proliferation (C–D) and apoptosis (E–F) of 16HBECs were compared among NC group, CSE group, miR-221-3p/miR-92a-3p mimic group, miR-221-3p/miR-92a-3p inhibitor group, CSE+miR-221-3p/miR-92a-3p mimic and CSE+miR-221-3p/miR-92a-3p inhibitor. * $p < 0.05$ when compared with NC group, # $p < 0.05$ when compared with miR-221-3p/miR-92a-3p mimic or inhibitor group

alone ($p < 0.05$) (Figures 6A,C and 7A,C). By contrast, expressions of TNF- α , IL-6, IL-1 β , TGF- β 1, Collagen IV, Fibronectin, and α -SMA were decreased prominently in 16HBECs of miR-221-3p/miR-92a-3p inhibitor+CSE group, when compared with CSE treatment group ($p < 0.05$) (Figures 6B,D and 7B,D).

4 | DISCUSSION

Smoking, a well-known external trigger of chronic COPD,²² increases likelihood of COPD onset by 2~4 times.²³ Harmful substances of cigarettes, including nicotine, nitric oxide, tar, aldehydes, phenols and hydrocyanic acid, serves to exacerbate airway inflammation²⁴ and promote apoptosis of airway epithelial cells,²⁵ thus facilitating occurrence of COPD. Hence, it was vital to expose the internal

connection of CSE with COPD development, so as to hinder COPD progression as much as possible.

Airway epithelium, a physiological barrier, is meant to protect respiratory system from harms of outside stimulants. Destroying its structural integrity could lead to necrosis of airway epithelial cells and overwhelming inflammation in the airway.²⁶ In this study, we observed that 16HBECs after CSE treatment were predisposed to apoptosis (Figure 4C), and they produced larger amounts of inflammatory cytokines, including TNF- α , IL-6, IL-1 β , and TGF- β 1, and airway remodeling biomarkers, including Collagen IV, Fibronectin and α -SMA, than 16HBECs treated by none (Figure 4D–E), which implied that airway epithelium might be injured by CSE. Regarding inflammatory factors investigated here, TNF- α and IL-1 β are up-regulated when inflammation cascade is initiated,^{27,28} and IL-6 level, mainly secreted by monocytes and macrophages, is prominently increased

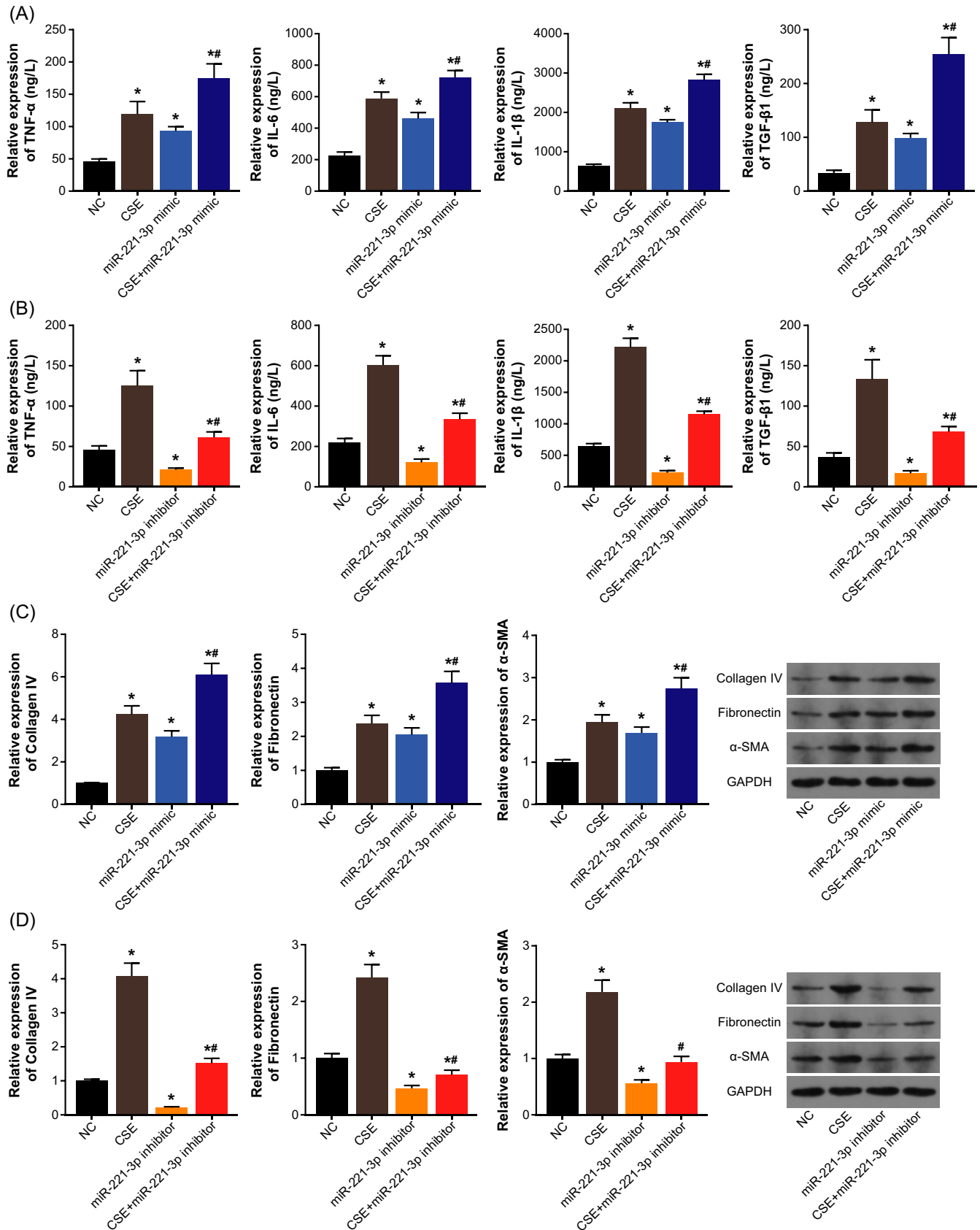


FIGURE 6 Expressions of inflammatory cytokines (A–B) and airway remodeling-associated proteins (C–D) were determined among 16HBECs of NC group, CSE group, miR-221-3p mimic group, miR-221-3p inhibitor group, CSE+miR-221-3p mimic and CSE+miR-221-3p inhibitor. * $p < 0.05$ when compared with NC group, # $p < 0.05$ when compared with miR-221-3p mimic or inhibitor group

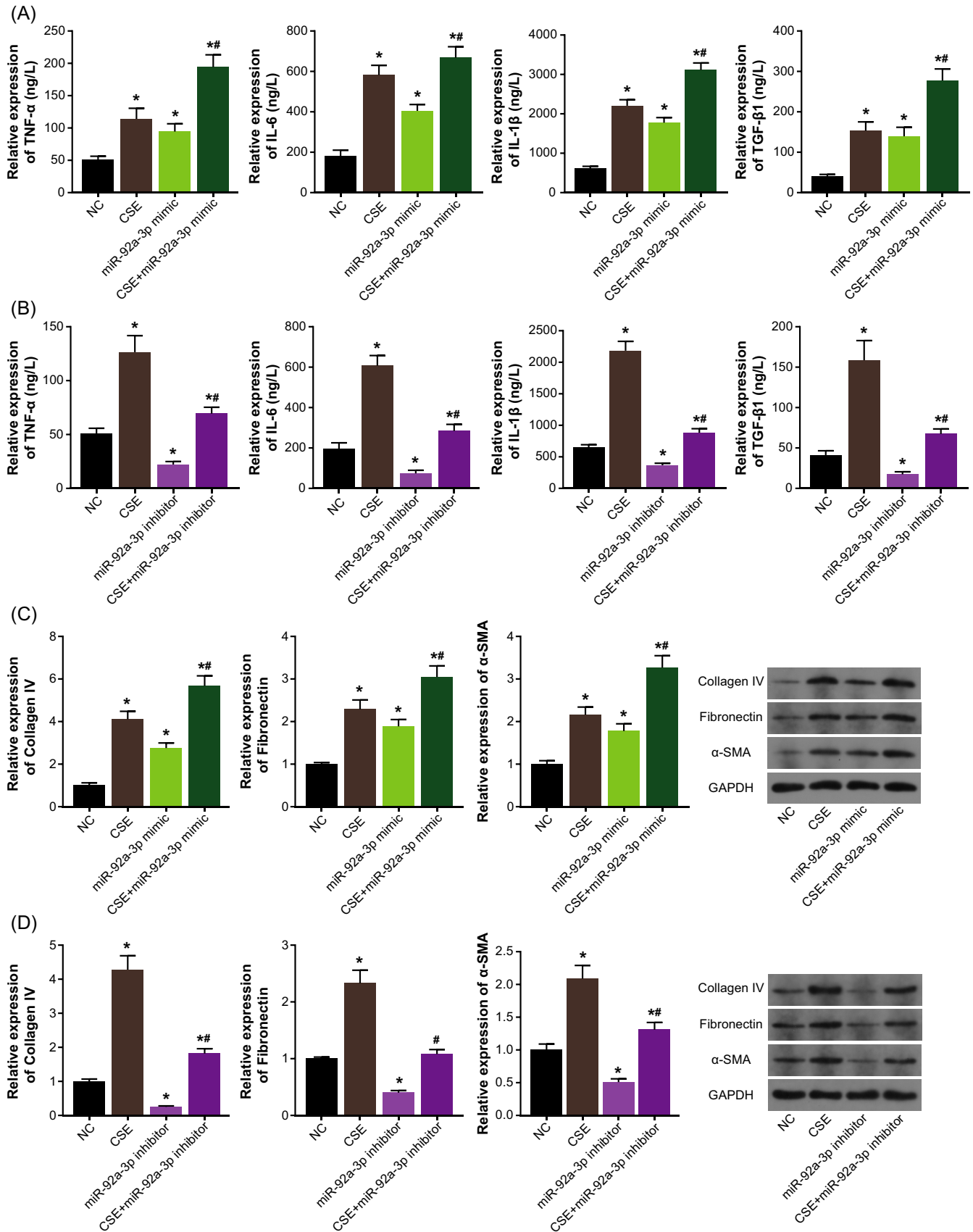


FIGURE 7 Expressions of inflammatory cytokines (A–B) and airway remodeling-associated proteins (C–D) were determined among 16HBECs of NC group, CSE group, miR-92a-3p mimic group, miR-92a-3p inhibitor group, CSE+miR-92a-3p mimic and CSE+miR-92a-3p inhibitor. * $p < 0.05$ when compared with NC group, # $p < 0.05$ when compared with miR-92a-3p mimic or inhibitor group

as inflammation severity of COPD escalates.²⁹ TGF- β 1, released by monocytes, expedites airway remodeling by promoting proliferation of airway smooth muscle cells,³⁰ which also explains why levels of airway remodeling biomarkers were increased in CSE-exposed 16HBECS (Figure 4E). Summing up the above, CSE was likely to stimulate damages in airway epithelium by pathologically inducing airway inflammation and airway remodeling.

Furthermore, a number of miRNAs have been corroborated to associate with smoking, for instance, miR-223 was under-expressed in the population accustomed to smoking as compared with people without such a habit,³¹ and miR-34a expression is markedly decreased in COPD mice models which were exposed to CSE.³² When it came to a Belgium cohort, miR-92a-3p, miR-218-5p, miR-221-3p, miR-99b-5p, and miR-34a-3p were profoundly over-expressed in lung tissues of COPD patients with smoking history.³³ Similarly, this investigation also revealed that serum levels of miR-221-3p and miR-92a-3p were dramatically increased in a Chinese COPD population with smoking history (Figure 1A). On top of that, detecting serum levels of miR-221-3p and miR-92a-3p was considered feasible in differentiating COPD patients of various severities (Figure 3). Although highly expressed miR-221 and miR-92a were also measurable in bronchial epithelial cells, lung tissues and plasma of asthma and lung cancer patients,³⁴⁻³⁶ the specificity of miR-221 and miR-92a in COPD diagnosis might not be reduced for that we focused on serum in this investigation. Despite this strength, combination with other biomarkers or association with clinical symptoms^{37,38} might yield more desirable results in COPD diagnosis than application of miR-221/miR-92a alone.

Mechanistically, inhibiting miR-221-3p/miR-92a-3p expression was beneficial to attenuate CSE-induced excessive inflammation in 16HBECS (Figures 6-7), which underlined the pro-inflammatory role of miR-221-3p and miR-92a-3p in smoking-induced COPD. In effect, the linkage of miR-221-3p/miR-92a-3p with inflammation-triggered lung injury and respiratory disorder has been emphasized numerously. For example, miR-221 facilitated lung injury by motivating NF- κ B signaling,³⁹ and accelerated asthmatic progression by worsening eosinophilic inflammation in the airway.⁴⁰ For another, miR-92a aggravated acute lung injury by mobilizing PTEN/AKT/NF- κ B signaling and increasing production of IL-6 and TNF- α .⁴¹ Nonetheless, downstream pathways that miR-221-3p and miR-92a-3p activated or deactivated to mediate smoking-facilitated COPD have not yet been comprehensively studied.

In addition to over-inflammation, apoptosis of 16HBECS, which was relevant to deterioration of lung injury,⁴² was facilitated by both miR-221-3p and miR-92a-3p (Figure 5). Consistent with this pro-apoptotic role, apoptosis of lung fibroblasts was promoted by miR-221-3p during progression of pneumonia,⁴³ and Wilms tumor cells became apoptotic under the influence of highly expressed miR-92a.⁴⁴ Certain investigations, however, appeared to draw contradictory results. To be specific, miR-221 was speculated to increase odds of tumorigenesis by curbing apoptosis of tumor cells in glioblastoma,⁴⁵ gastric cancer,⁴⁶ pancreatic cancer,⁴⁷ papillary thyroid carcinoma⁴⁸ and acute myelogenous leukemia.⁴⁹ And the

proliferative capability of neoplastic cells, including colorectal cancer cells,⁵⁰ cervical cancer cells,⁵¹ pancreatic cancer cells,⁵² breast cancer cells⁵³ and ovarian cancer cells, was reinforced by highly expressed miR-92a. We ascribed this controversy to that miR-221-3p and miR-92a-3p might play discrepant roles in cell types with disparate pathological mechanisms.

In conclusion, miR-221-3p and miR-92a-3p were both implicated in CSE-caused inflammation disorder underlying pathogenesis of COPD, and they were promising biomarkers in the diagnosis of COPD. However, there were several defects in the experimental design. Firstly, animal models of COPD were not constructed, so that the in-vivo effects of miR-221-3p and miR-92a-3p on tobacco-induced inflammation could not be validated. Secondly, the molecular network that explained roles of miR-221-3p and miR-92a-3p in COPD was hitherto not all-sided. Finally, COPD patients recruited were all of Chinese Han ethnicity, so conclusions of this study might not go for populations of other ethnicities. To settle puzzles as mentioned above, more studies with rigorous designs were in need.

ACKNOWLEDGEMENTS

None

CONFLICT OF INTEREST

None.

DATA AVAILABILITY STATEMENT

All data generated or analyzed during this study are included in this article.

ORCID

Guixian Song  <https://orcid.org/0000-0002-5208-4811>

REFERENCES

1. Cui H, Ge J, Xie N, et al. miR-34a promotes fibrosis in aged lungs by inducing alveolarepithelial dysfunction. *Am J Physiol Lung Cell Mol Physiol*. 2017;312:L415-L424.
2. Boulet LP, FitzGerald JM, Reddel HK. The revised 2014 GINA strategy report: opportunities for change. *Curr Opin Pulm Med*. 2015;21:1-7.
3. Shahriary A, Ghanei M, Rahmani H. The systemic nature of mustard lung: comparison with COPD patients. *Interdiscip Toxicol*. 2017;10:114-127.
4. Firoozabadi MD, Sheikhi MA, Rahmani H, et al. Risks of on-pump coronary artery bypass grafting surgery in patients with chronic obstructive pulmonary disease due to sulfur mustard. *Postepy Dermatol Alergol*. 2017;34:429-432.
5. Shahriary A, Panahi Y, Shirali S, et al. Relationship of serum levels of interleukin 6, interleukin 8, and C-reactive protein with forced expiratory volume in first second in patients with mustard lung and chronic obstructive pulmonary diseases: systematic review and meta-analysis. *Postepy Dermatol Alergol*. 2017;34:192-198.
6. Osei ET, Florez-Sampedro L, Timens W, et al. Unravelling the complexity of COPD by microRNAs: it's a small world after all. *Eur Respir J*. 2015;46:807-818.
7. Huang C, Xie M, He X, et al. Activity of sputum p38 MAPK is correlated with airway inflammation and reduced FEV1 in COPD patients. *Med Sci Monit*. 2013;19:1229-1235.

8. Rom O, Avezov K, Aizenbud D, et al. Cigarette smoking and inflammation revisited. *Respir Physiol Neurobiol*. 2013;187:5-10.
9. Li B, Lu Y, Wang H, et al. miR-221/222 enhance the tumorigenicity of human breast cancer stem cells via modulation of PTEN/Akt pathway. *Biomed Pharmacother*. 2016;79:93-101.
10. Zhao D, Zhuang N, Ding Y, et al. MiR-221 activates the NF-kappaB pathway by targeting A20. *Biochem Biophys Res Commun*. 2016;472:11-18.
11. Knyazev EN, Mal'tseva DV, Zakharyants AA, et al. Expression of microRNA Genes MIR221, MIR222, and MIR181B1 increases during induction of inflammation in the endothelial barrier model. *Bull Exp Biol Med*. 2018;164:749-752.
12. Ghobadi H, Aslani MR, Hosseini A, et al. The correlation of serum brain natriuretic peptide and interleukin-6 with quality of life using the chronic obstructive pulmonary disease assessment test. *Med Princ Pract*. 2017;26:509-515.
13. Inui T, Watanabe M, Nakamoto K, et al. Bronchial epithelial cells produce CXCL1 in response to LPS and TNFalpha: a potential role in the pathogenesis of COPD. *Exp Lung Res*. 2018;44:323-331.
14. Peng J, Zhou Y, Deng Z, et al. miR-221 negatively regulates inflammation and insulin sensitivity in white adipose tissue by repression of sirtuin-1 (SIRT1). *J Cell Biochem*. 2018;119:6418-6428.
15. Loyer X, Potteaux S, Vion AC, et al. Inhibition of microRNA-92a prevents endothelial dysfunction and atherosclerosis in mice. *Circ Res*. 2014;114:434-443.
16. Rong X, Jia L, Hong L, et al. Serum miR-92a-3p as a new potential biomarker for diagnosis of kawasaki disease with coronary artery lesions. *J Cardiovasc Transl Res*. 2017;10:1-8.
17. Daniel JM, Penzkofer D, Teske R, et al. Inhibition of miR-92a improves re-endothelialization and prevents neointima formation following vascular injury. *Cardiovasc Res*. 2014;103:564-572.
18. Fu F, Jiang W, Zhou L, et al. Circulating exosomal miR-17-5p and miR-92a-3p predict pathologic stage and grade of colorectal cancer. *Transl Oncol*. 2018;11:221-232.
19. Wang WY, Zheng YS, Li ZG, et al. MiR-92a contributes to the cardiovascular disease development in diabetes mellitus through NF-kappaB and downstream inflammatory pathways. *Eur Rev Med Pharmacol Sci*. 2019;23:3070-3079.
20. Semba RD, Chang SS, Sun K, et al. Serum 25-hydroxyvitamin D and pulmonary function in older disabled community-dwelling women. *J Gerontol A Biol Sci Med Sci*. 2012;67:683-689.
21. Krimmer DI, Burgess JK, Wooi TK, et al. Matrix proteins from smoke-exposed fibroblasts are pro-proliferative. *Am J Respir Cell Mol Biol*. 2012;46:34-39.
22. Kurmi OP, Li L, Wang J, et al. COPD and its association with smoking in the Mainland China: a cross-sectional analysis of 0.5 million men and women from ten diverse areas. *Int J Chron Obstruct Pulmon Dis*. 2015;10:655-665.
23. Tzanakis N, Anagnostopoulou U, Filaditaki V, et al. Prevalence of COPD in Greece. *Chest*. 2004;125:892-900.
24. Crotty Alexander LE, Drummond CA, Hepokoski M, et al. Chronic inhalation of e-cigarette vapor containing nicotine disrupts airway barrier function and induces systemic inflammation and multiorgan fibrosis in mice. *Am J Physiol Regul Integr Comp Physiol*. 2018;314:R834-R847.
25. West KA, Brognard J, Clark AS, et al. Rapid Akt activation by nicotine and a tobacco carcinogen modulates the phenotype of normal human airway epithelial cells. *J Clin Invest*. 2003;111:81-90.
26. Lambrecht BN, Hammad H. The airway epithelium in asthma. *Nat Med*. 2012;18:684-692.
27. Kubysheva N, Boldina M, Eliseeva T, et al. Relationship of serum levels of IL-17, IL-18, TNF-alpha, and lung function parameters in patients with COPD, asthma-COPD overlap, and bronchial asthma. *Mediators Inflamm*. 2020;2020:4652898.
28. Peng Z, Zhang W, Qiao J, et al. Melatonin attenuates airway inflammation via SIRT1 dependent inhibition of NLRP3 inflammasome and IL-1beta in rats with COPD. *Int Immunopharmacol*. 2018;62:23-28.
29. Gorska K, Nejman-Gryz P, Paplinska-Goryca M, et al. Comparative study of IL-33 and IL-6 levels in different respiratory samples in mild-to-moderate asthma and COPD. *COPD*. 2018;15:36-45.
30. Chen M, Lv Z, Huang L, et al. Triptolide inhibits TGF-beta1-induced cell proliferation in rat airway smooth muscle cells by suppressing Smad signaling. *Exp Cell Res*. 2015;331:362-368.
31. Micolucci L, Akhtar MM, Olivieri F, et al. Diagnostic value of microRNAs in asbestos exposure and malignant mesothelioma: systematic review and qualitative meta-analysis. *Oncotarget*. 2016;7:58606-58637.
32. Booton R, Lindsay MA. Emerging role of MicroRNAs and long non-coding RNAs in respiratory disease. *Chest*. 2014;146:193-204.
33. Conickx G, Mestdagh P, Avila Cobos F, et al. MicroRNA profiling reveals a role for microRNA-218-5p in the pathogenesis of chronic obstructive pulmonary disease. *Am J Respir Crit Care Med*. 2017;195:43-56.
34. Zhang H, Sun Y, Rong W, et al. miR-221 participates in the airway epithelial cells injury in asthma via targeting SIRT1. *Exp Lung Res*. 2018;44:272-279.
35. Yin G, Zhang B, Li J. miR2213p promotes the cell growth of nonsmall cell lung cancer by targeting p27. *Mol Med Rep*. 2019;20:604-612.
36. Xu X, Zhu S, Tao Z, et al. High circulating miR-18a, miR-20a, and miR-92a expression correlates with poor prognosis in patients with non-small cell lung cancer. *Cancer Med*. 2018;7:21-31.
37. Maselli DJ, Bhatt SP, Anzueto A, et al. Clinical epidemiology of COPD: insights from 10 years of the COPD Gene study. *Chest*. 2018;44:228-238.
38. Ferment JM, Masconi KL, Jensen MT, et al. Biomarkers and clinical outcomes in COPD: a systematic review and meta-analysis. *Thorax*. 2019;74:439-446.
39. Wang T, Jiang L, Wei X, et al. Inhibition of miR-221 alleviates LPS-induced acute lung injury via inactivation of SOCS1/NF-kappaB signaling pathway. *Cell Cycle*. 2019;18:1893-1907.
40. Zhang K, Liang Y, Feng Y, et al. Decreased epithelial and sputum miR-221-3p associates with airway eosinophilic inflammation and CXCL17 expression in asthma. *Am J Physiol Lung Cell Mol Physiol*. 2018;315:L253-L264.
41. Xu F, Zhou F. Inhibition of microRNA-92a ameliorates lipopolysaccharide-induced endothelial barrier dysfunction by targeting ITGA5 through the PI3K/Akt signaling pathway in human pulmonary microvascular endothelial cells. *Int Immunopharmacol*. 2020;78:106060.
42. Ng CS, Wan S, Yim AP. Pulmonary ischaemia-reperfusion injury: role of apoptosis. *Eur Respir J*. 2005;25:356-363.
43. Wang C, Qu Z, Kong L, et al. Quercetin ameliorates lipopolysaccharide-caused inflammatory damage via down-regulation of miR-221 in WI-38 cells. *Exp Mol Pathol*. 2019;108:1-8.
44. Zhu S, Zhang L, Zhao Z, et al. MicroRNA92a3p inhibits the cell proliferation, migration and invasion of Wilms tumor by targeting NOTCH1. *Oncol Rep*. 2018;40:571-578.
45. Ciafre SA, Galardi S, Mangiola A, et al. Extensive modulation of a set of microRNAs in primary glioblastoma. *Biochem Biophys Res Commun*. 2005;334:1351-1358.
46. Pineau P, Volinia S, McJunkin K, et al. miR-221 overexpression contributes to liver tumorigenesis. *Proc Natl Acad Sci USA*. 2010;107:264-269.
47. Galardi S, Mercatelli N, Giorda E, et al. miR-221 and miR-222 expression affects the proliferation potential of human prostate carcinoma cell lines by targeting p27Kip1. *J Biol Chem*. 2007;282:23716-23724.
48. Yang Z, Yuan Z, Fan Y, et al. Integrated analyses of microRNA and mRNA expression profiles in aggressive papillary thyroid carcinoma. *Mol Med Rep*. 2013;8:1353-1358.

49. Rommer A, Steinleitner K, Hackl H, et al. Overexpression of primary microRNA 221/222 in acute myeloid leukemia. *BMC Cancer*. 2013;13:364.
50. Zhou T, Zhang G, Liu Z, et al. Overexpression of miR-92a correlates with tumor metastasis and poor prognosis in patients with colorectal cancer. *Int J Colorectal Dis*. 2013;28:19-24.
51. Zhou C, Shen L, Mao L, et al. miR-92a is upregulated in cervical cancer and promotes cell proliferation and invasion by targeting FBXW7. *Biochem Biophys Res Commun*. 2015;458:63-69.
52. Tian L, Fang YX, Xue JL, et al. Four microRNAs promote prostate cell proliferation with regulation of PTEN and its downstream signals in vitro. *PLoS One*. 2013;8:e75885.
53. Si H, Sun X, Chen Y, et al. Circulating microRNA-92a and microRNA-21 as novel minimally invasive biomarkers for primary breast cancer. *J Cancer Res Clin Oncol*. 2013;139:223-229.

SUPPORTING INFORMATION

Additional supporting information may be found online in the Supporting Information section.

How to cite this article: Shen Y, Lu H, Song G. MiR-221-3p and miR-92a-3p enhances smoking-induced inflammation in COPD. *J Clin Lab Anal*. 2021;35:e23857. <https://doi.org/10.1002/jcla.23857>